

UNSTEADY VORTEX BREAKDOWN IN AN ENCLOSED CYLINDER FLOW

J.M. LOPEZ

Aeronautical Research Laboratory
 P.O. Box 4331, Melbourne, Vic. 3001
 AUSTRALIA

INTRODUCTION

In certain parameter regimes the confined swirling flow generated inside an enclosed cylinder by the constant rotation of one of its endwalls manifests itself as a steady axisymmetric vortex breakdown. This system, which is well posed mathematically with respect to the boundary conditions, is fully specified by two non-dimensional parameters. These are the aspect ratio of the cylinder H/R , where H is the height and R is the radius of the cylinder, and the Reynolds number $Re = \Omega R^2/\nu$, where Ω is the constant angular speed of the rotating endwall and ν is the kinematic viscosity (see Figure 1).

The basic features of the flow are as follows. The fluid, which completely fills the cylinder, is initially at rest. At $t = 0$, the bottom endwall is impulsively set to rotate at constant angular speed Ω . An Ekman boundary layer develops on the rotating disk with thickness of order $Re^{-0.5}$. This rotating boundary layer acts as a centrifugal pump, sending fluid radially outwards in a spiralling motion while drawing fluid into it from above. This pumping action, together with the presence of the cylinder sidewall, sets up a secondary meridional circulation. In time, typically of the

order of one hundred endwall rotations, fluid with angular momentum and dynamic head acquired in the Ekman layer, reaches the vicinity of the top endwall, where it is deflected towards the centre. It spirals inwards creating a further boundary layer on the top endwall. On this endwall, the flow separates at $r = 0$ and spirals back down towards the rotating endwall, forming a concentrated central vortex.

Experimental investigations (eg. Vogel 1968, Escudier 1984) have demonstrated that for $Re < 10^8$, the flow is steady and that the secondary meridional flow has streamlines with monotonic curvature. In a cylindrical co-ordinate system with the origin at the center of the rotating endwall, this means that the azimuthal component of vorticity, η , associated with the simple overturning meridional flow is negative. Above a critical Re , which depends on H/R , the experiments have shown that the streamtubes become wavy and at higher Re the flow on the axis stagnates and leads to the formation of one or more steady axisymmetric vortex breakdown bubbles. Lopez (1988) obtained numerical solutions of the axisymmetric Navier-Stokes equations for this flow. These show that the transition to breakdown in the flow is associated with the generation of a positive azimuthal component of vorticity through the tilting and stretching of the vorticity associated with the central vortex. This vorticity vector field primarily consists of a negative component in the vertical direction, due to the spiralling motion down towards the Ekman layer, and a negative azimuthal component due to the meridional overturning flow. In Brown & Lopez (1988) this vortex deformation mechanism was investigated analytically by considering an inviscid swirling flow. It was found that for such a flow, wavy solutions, and hence vortex breakdown, are possible as a result of vortex deformation when the helix angle of the velocity vector is greater than that of the vorticity vector, the helix angle of a vector being the ratio of its azimuthal to vertical components.

Beyond a second critical Re , again dependent upon H/R , the flow undergoes a further transition from an axisymmetric steady state to an axisymmetric periodic state. The only experimental results presently available in this regime are Escudier's (1984), where he has mapped out this transition in $Re - H/R$ parameter space for $1.5 < H/R < 3.5$, and has presented flow visualization for the case $Re = 2765$, $H/R = 2.5$. Escudier concludes that for values of Re just above the curve separating the steady and unsteady regimes in $Re - H/R$ space, the oscillation is periodic and axial; and that as Re is increased the motion becomes disturbed and ultimately turbulent.

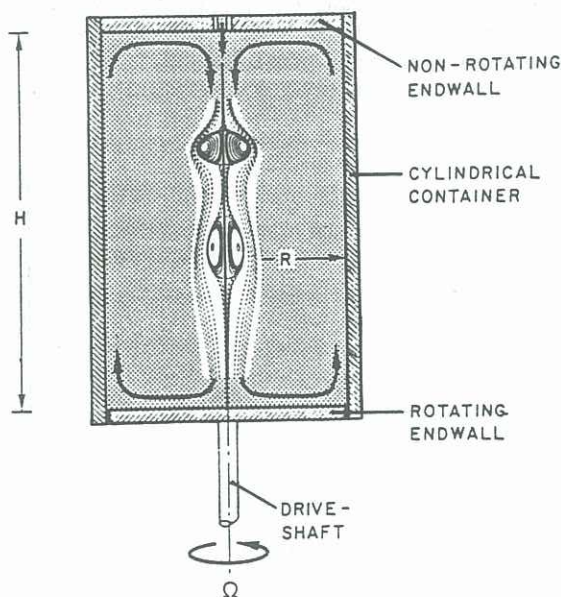


FIGURE 1: A slice through the meridional plane of the cylinder flow with a schematic of a two bubble vortex breakdown in the central core.

In this study, the transitions in flow states as Re is increased are investigated for the case of $H/R = 2.5$, which has a richness of flow phenomena leading to chaos at high Re , where Re may be regarded as a parameterised measure of the driving force of this system. The Ruelle, Takens & Newhouse (1978) scenario for the transition to chaos as a driving force parameter increases, typically exhibits a parameter range where the system has steady state solutions. As the parameter is increased, there is a transfer of stability from steady state to limit cycle solutions. A further increase in the parameter leads to a transfer in stability from the periodic solution set to quasi-periodic solutions with two incommensurate frequencies. The two-dimensional torus, on which the quasi-periodic solutions are stable, may lose stability with a further increase in the parameter. It may be replaced with motion on a three-dimensional torus or become chaotic, exhibiting broadband spectral excitation. The $H/R = 2.5$ numerical sequence, as Re is increased, follows a route to chaos which very closely follows the Ruelle-Takens-Newhouse scenario.

Due to the limited experimental data and the lack of any stability analysis for the unsteady flow, we have little feeling for the stability of our solutions to asymmetric disturbances, be they finite amplitude or infinitesimal. The experiments of Escudier (1984) at least demonstrate that the steady solutions are stable to infinitesimal perturbations. Roesner (private communication) has shown experimentally that small, but finite amplitude perturbations, such as a slight wobble in the disk at some Re below the critical steady—periodic value in the unperturbed case, leads to a transition from the steady axisymmetric state to an asymmetric periodic state in which the breakdown bubble is seen to precess around the axis. The numerical model does not account for any of these types of solutions and in fact, the axisymmetric solutions at the higher Re are expected to be unstable to infinitesimal disturbances of this nature leading to a fully three-dimensional flow. However, even with the limitation of axial symmetry, our simple model is of interest in providing insight into the physical mechanisms driving the flow from steady state through the unsteady regimes into chaos, in the absence of any asymmetric disturbances. Despite the axisymmetric restriction, the model is not as restrictive as a planar two-dimensional study of transition to non-periodic flow. The swirling axisymmetric system has three non-zero orthogonal components of velocity and vorticity and hence allows for the tilting and stretching of vorticity.

SYSTEM OF EQUATIONS AND METHOD OF SOLUTION

The numerical model consists of the axisymmetric Navier-Stokes equations in conservative streamfunction-vorticity form, with time and length scaled by $1/\Omega$ and R respectively. These are solved using an explicit finite-difference scheme, detailed in Lopez (1988) where the accuracy of the method is also discussed.

The transition from the periodic to chaotic state will be illustrated by focusing on six solutions at representative values of Re . The transition from steady to periodic flow has been covered in Lopez (1989) and will only be discussed briefly here.

Power spectra, computed from the squared modulus of the fast Fourier transform of the axial velocity at the centre of the cylinder (i.e. $r = 0$, $z = H/2R$) using standard discrete techniques, are used to identify the various tran-

sitions as Re is increased. Spectral estimates are obtained at frequency intervals of $\Delta f = 1/N\Delta t$, where for the 'low' Re cases (i.e. $Re = 3 \times 10^3$, 3.5×10^3 , 4×10^3 & 6×10^3), $N = 2^{16}$ and $\Delta t = 0.05$; and for the 'high' Re cases (i.e. $Re = 10^4$ & 2×10^4), $N = 2^{16}$ and $\Delta t = 0.025$. In all cases, the first 1,350 endwall rotations (i.e. 27,000 and 54,000 time-steps for the 'low' and 'high' Re cases respectively) are not used in the spectral analysis to avoid the transient oscillations from the impulsive start-up. For all cases considered, the spectral resolution between spectral estimates is approximately 6×10^{-4} . The Nyquist frequency $f_N = 1/2\Delta t$, is 10 and 20 for the 'low' and 'high' Re cases, giving frequency resolutions $\Delta f/f_N$ of 2^{-14} and 2^{-15} respectively.

RESULTS AND DISCUSSION

For the case of aspect ratio $H/R = 2.5$, the numerical results of Lopez (1988, 1989) show that the first bifurcation of the flow as Re is increased occurs at about $Re = 1.6 \times 10^3$ and corresponds to a small amplitude standing wave on the central vortex core at steady state. As Re is increased from 1.6×10^3 to 2.6×10^3 Escudier's (1984) experimental results and Lopez' (1988, 1989) numerical results demonstrate that the flow undergoes a further steady bifurcation where the flow stagnates on the axis of symmetry at $Re \approx 1.9 \times 10^3$. This new flow state consists of a steady axisymmetric vortex breakdown with two recirculation bubbles on the axis, similar to that shown schematically in Figure 1.

As Re is increased further, the centrifugal standing wave on the vortex core increases in amplitude and decreases in wavelength. A transient oscillation has always been observed to follow the impulsive start. The characteristic frequency of this transient is $f_0 \approx 0.0175$ and for $H/R = 2.5$, f_0 is independent of Re and damped. A number of cases have been computed at $Re = 3 \times 10^3$ for various H/R and it has been found that for $H/R < 2$, this f_0 oscillation is not damped but settles to a periodic limit cycle. The characteristic frequency f_0 increases smoothly as H/R is decreased from about 3. At larger H/R the flow is steady. At $H/R = 1$ the flow consists of a standing wave, and f_0 becomes asymptotically large as H/R approaches one from above (see Figure 2).

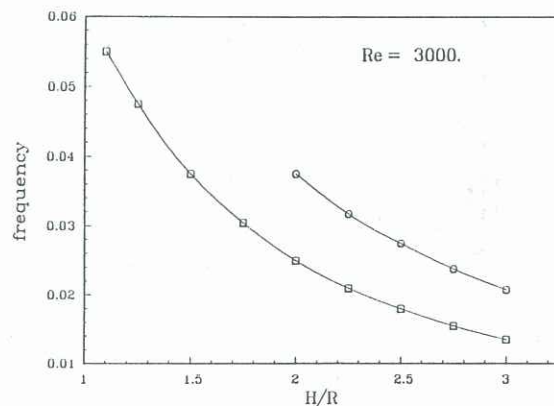


FIGURE 2: Frequency dependencies of oscillatory solutions on cylinder aspect ratio, H/R , for the case $Re = 3 \times 10^3$. □ — f_0 , ○ — f_1 . Where frequencies exist for the same H/R , the lower one is damped.

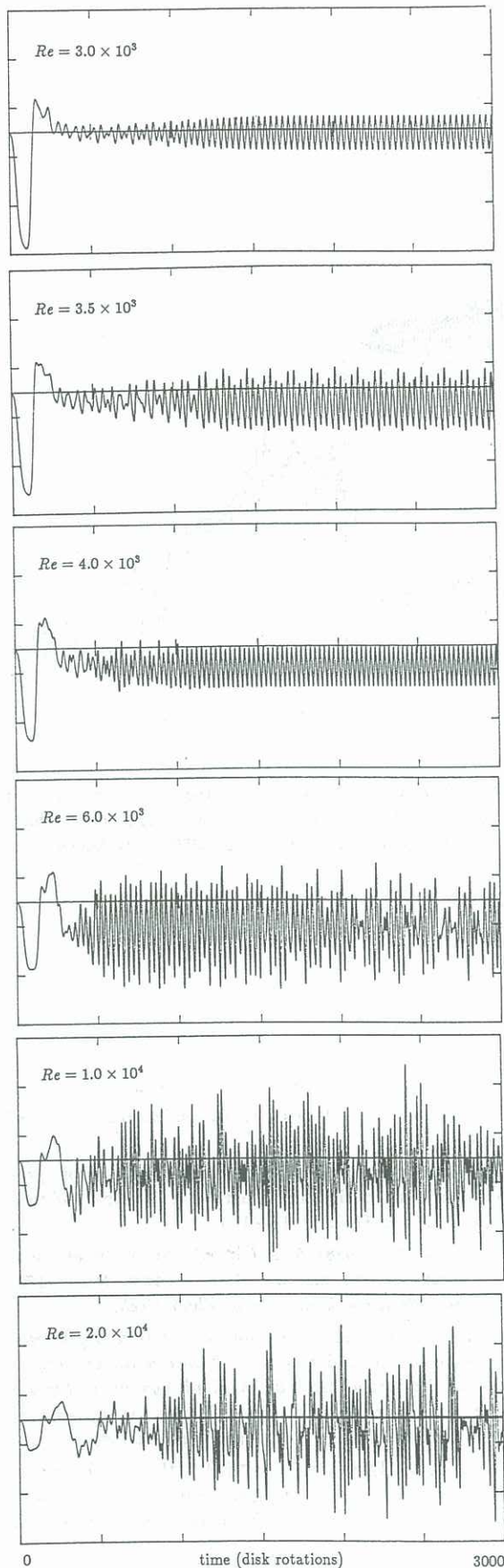


FIGURE 3: Time histories of the axial velocity at $r = 0$, $z = H/2R$, for $H/R = 2.5$ and Re as indicated.

Returning to the $H/R = 2.5$ situation, it is found that at $Re \approx 2.4 \times 10^3$, the two breakdown bubbles on the axis have coalesced. At about $Re = 2.6 \times 10^3$, the system undergoes a Hopf bifurcation to a limit cycle solution with characteristic frequency $f_1 \approx 0.0275$, following the damping of the transient f_0 oscillations. This f_1 oscillation is clearly seen as an interaction between the two bubbles and is limited primarily to the central core region. In Figure 3, the time history of the axial component of the velocity at the centre of the cylinder $w(r = 0, z = H/2R)$, shows the initial transient over-shoot following the impulsive start and the resultant f_0 oscillations beginning after about 20 disk rotations. At $t \approx 50$, the time history shows the growth of a new oscillation, which by $t = 1500$ has settled to a steady limit cycle and the f_0 oscillations have been damped. The power spectra for this signal in Figure 4 has very sharp spikes at f_1 , $2f_1$ and $3f_1$, together with very faint lobes at f_0 , $2f_1 - f_0$ and $f_1 + f_0$. These faint signals associated with f_0 are expected to disappear at later times. Note that all spectra reported here are taken from $t = 1350$ to $t = 2988.4$.

The physical mechanism responsible for this f_1 oscillation seems to be the coalescing of the two breakdown bubbles resulting in one larger bubble. This large bubble then appears to alter the upstream flow in such a way that the vortex deformation mechanism discussed in the introduction can no longer maintain this oversized combined bubble. The meridional flow then has a dominant influence over this region of the flow and begins to wash the large bubble downstream. In doing so, the recirculating bubble flow is weakened, the central vortex reforms and the vortex deformation mechanism re-establishes itself. This then leads to a new breakdown being formed and the old breakdown, which is drawn upstream, coalesces with the new upstream bubble. This whole process is repeated with frequency f_1 .

From Figures 3 and 4, we find that at $Re \approx 3.5 \times 10^3$, there is a mode competition and that at $Re \approx 4 \times 10^3$ the new mode is dominant. This new mode has a characteristic frequency $f_2 \approx 0.033$. The spectra at $Re = 3.5 \times 10^3$ is of a quasi-periodic flow with sharp spikes at $m_1 f_1 + m_2 f_2$, m_1 and m_2 being integer, whereas at $Re = 4 \times 10^3$ the spectra once again corresponds to a periodic limit cycle with peaks at f_2 and $2f_2$. In the spectra shown in Figure 4, there is still a faint signal due to f_1 which has not been completely damped in the time interval used to obtain the spectra.

The mechanism for this new mode is basically the same as for the f_1 mode, except that now the meridional flow carries the 'dead' bubble downstream faster than the vortex core can reform to create a new breakdown region and draw the 'dead' bubble back upstream. This washing away of the 'dead' bubble and the formation of a new bubble occurs at the new frequency f_2 . In the $Re = 3.5 \times 10^3$ case, the 'dead' bubble is also washed away, but it feels the influence of the new bubble forming and so has a jerky journey downstream, leading to the non-linear spectra.

As Re is increased to 6×10^3 , the flow becomes non-periodic and the spectrum is marked by broadband components, particularly at the lower frequencies. The flow can no longer be described by a small number of well defined characteristic frequencies; it is said to be chaotic or weakly turbulent. Note however, that the spectrum still consists of sharp peaks representing the fundamental frequency $f_2 \approx 0.033$ and a new frequency $f_3 \approx 0.038$ and their linear combinations. Also, the flow is still highly

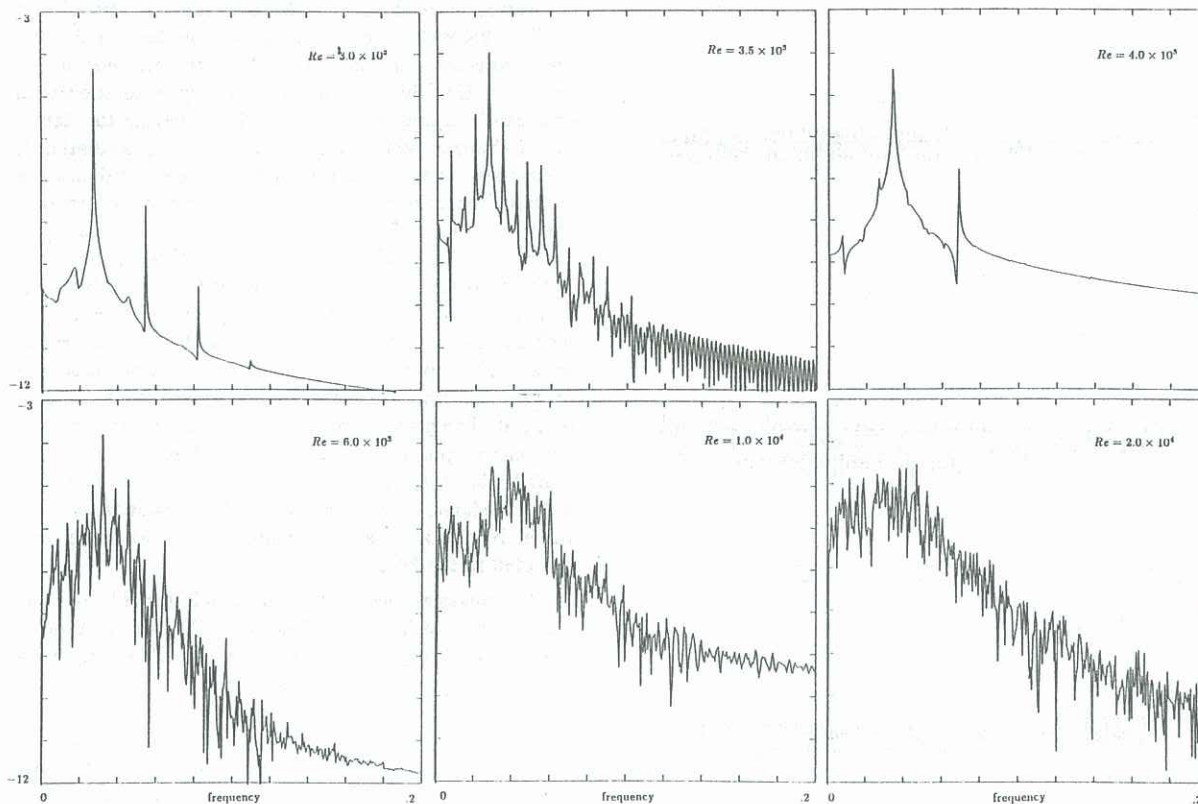


FIGURE 4: Power spectra (plotted in semi-log form) of the time histories shown in Figure 3. The spectra have been taken over the time interval $1350 \leq t \leq 2988.4$.

ordered spatially. Nevertheless, there has been a qualitative change in the behaviour of the system due to the appearance of the broadband components and hence accurate predictions of the flow field variables based on solutions at earlier times in the evolution can no longer be made. The majority of the spectra may correspond to motion on a three-dimensional torus with frequency response $m_1 f_1 + m_2 f_2 + m_3 f_3$, but it is difficult to ascertain this with any reasonable accuracy.

However, when Re is increased to 10^4 , the spectra is broadband with the high frequencies (not shown) obeying a power law relationship. At $Re = 10^4$, one can still pick out $m_1 f_2 + m_2 f_3$ spikes, albeit with some difficulty. But at $Re = 2 \times 10^4$ the low frequency spectra is nearly flat with no dominant frequency discernable.

The mechanism which leads to this new f_3 mode is found from the close examination of the entire flow field as it evolves. At $Re = 6 \times 10^3$, the boundary layer on the cylinder sidewall separates, forming a small separation ring on the sidewall which spirals upwards and is then ejected into the interior of the flow as it nears the top of the cylinder. This relatively small scale eddy follows an irregular path towards the central vortex region where it interacts weakly with the f_1 and f_2 modes of oscillation. The boundary layer separation occurs irregularly, but by examining the velocity one grid point away from the sidewall (i.e. $r = 59/60$), a minimum in the axial velocity occurs with a frequency of approximately f_3 (≈ 0.038), which suggests that the onset of the chaotic behaviour is due to the sidewall boundary layer separation. The precise mechanism responsible for the boundary layer separation has not yet been discerned and is the subject of further study.

REFERENCES

- BROWN, G. L. & LOPEZ, J. M. (1988) Axisymmetric vortex breakdown. Part II: physical mechanisms. *A. R. L. Aero. Report 174*, AR-004-573; also submitted to *J. Fluid Mech.*
- ESCUDIER, M. P. (1984) Observations of the flow produced in a cylindrical container by a rotating endwall. *Experiments in Fluids* **2**, 189-196.
- LOPEZ, J. M. (1988) Axisymmetric vortex breakdown. Part I: confined swirling flow. *A. R. L. Aero. Report 173*, AR-004-572; also submitted to *J. Fluid Mech.*
- LOPEZ, J. M. (1989) Axisymmetric vortex breakdown in an enclosed cylinder flow. *11th International Conference on Numerical Methods in Fluid Dynamics, Lecture Notes in Physics 323*, pp. 384-388. (eds. D. L. Dwoyer, M. Y. Hussaini & R. G. Voigt) (Springer-Verlag).
- RUELLE, D., TAKENS, F. & NEWHOUSE, S. E. (1978) Occurrence of strange axiom A attractors near quasi-periodic flows on T^m , $m \geq 3$. *Commun. Math. Phys.* **64**, 35-40.
- VOGEL, H. U. (1968) Experimentelle Ergebnisse über die laminare Strömung in einen zylindrischen Gehäuse mit darin rotierender Scheibe. *Max-Planck-Inst. Bericht* **6**.